

Integration of benzocyclobutene polymers and silicon micromachined structures using anisotropic wet etching

Nima Ghalichechian, Alireza Modafe, and Reza Ghodssi^{a)}

*MEMS Sensors and Actuators Lab, Department of Electrical and Computer Engineering,
The Institute for Systems Research, University of Maryland, College Park, Maryland 20742*

Paolo Lazzeri, Victor Micheli, and Mariano Anderle

ITC-irst Centro per la Ricerca Scientifica e Tecnologica, 38050 Povo, Trento, Italy

(Received 23 April 2004; accepted 5 July 2004; published 13 October 2004)

Integration of thick, low- k dielectric benzocyclobutene (BCB) film with deep etched structures in silicon allows the fabrication of microelectromechanical systems (MEMS) devices with low parasitic loss. A fabrication process is developed for integration of 1- μm -thick BCB low- k dielectric film and 200- μm -deep anisotropically etched grooves in silicon with potassium hydroxide (KOH). In order to protect the low- k film during the highly corrosive, long, high-temperature KOH etching process, gold (Au) is used as an etch mask. Chromium (Cr) is used to improve the adhesion of Au to the underlying BCB layer. Metal-BCB adhesion is the key parameter in this masking design. Partial cure of BCB at 210 °C for 40 min with appropriate surface treatment (adhesion promoter) prior to metallization and full cure at 250 °C for 1 h after metallization, together with Cr/Au sputtering at 200 °C, improves the adhesion dramatically. The adhesion strength of metal films to BCB was experimentally verified in a qualitative manner. V grooves were etched into silicon in 20 wt%, 80 °C KOH solution for 8 h in the presence of 1 μm BCB film. BCB was protected and kept intact with an Au mask layer during the etch process. In order to understand the mechanism of the adhesion improvement, the interface between BCB and the Cr/Au layer was studied using secondary ion mass spectroscopy and Auger electron spectroscopy. Adhesion improvement which is mainly due to cure management and use of adhesion promoter is associated with (1) the diffusion of silicon and carbon from the polymer structure into the Cr layer, and (2) the chemical interaction of BCB and Cr at the interface mainly in the form of the oxidation of Cr. The integration of BCB and the KOH etching process which was obtained by improving the adhesion of metal etch mask to the BCB film, together with the study of the interfaces, allow us to use thick low dielectric constant BCB film for fabrication of MEMS devices with very low parasitic loss. © 2004 American Vacuum Society. [DOI: 10.1116/1.1787519]

I. INTRODUCTION

New materials for microelectromechanical systems (MEMS) and microsystems enable design and fabrication of microdevices and structures with enhanced features like highly efficient electric micromachines. Spin-on benzocyclobutene-based polymers (BCB),^{1,2} with dielectric constant of $k=2.65$, are promising candidates as low- k insulating materials in MEMS. The main advantage of BCB over the most widely used dielectric material, plasma enhanced chemical vapor deposited silicon dioxide (PECVD SiO₂), is the ability to deposit a thick layer (up to 50 μm) with a lower dielectric constant to reduce parasitic capacitance, which is proportional to dielectric constant and inversely proportional to film thickness. BCB exhibits much lower residual stress and a higher level of planarization than PECVD SiO₂, making it attractive for MEMS applications. BCB is also a spin-on material which makes its deposition process simpler than conventional chemical vapor deposition (CVD) pro-

cesses used for dielectric films like silicon dioxide and silicon nitride. The deposition process is completed with a cure step at relatively low temperature (250 °C).

CYCLOTENE™ is a spin-on, low- k dielectric from Dow Chemical (Midland, MI) based on the BCB polymer with a wide range of achievable thicknesses. CYCLOTENE was primarily developed as an inter-level dielectric and passivation coating in microelectronic interconnects.^{3,4} It has been used in multichip module packaging,^{5,6} flip-chip solder bumping,^{7,8} Damascene copper (Cu) interconnects,⁹ as a stress buffer and passivation layer,¹⁰ as an insulating dielectric in rf high- Q inductors,¹¹ and for optical waveguides.^{12,13} Humidity sensors,¹⁴ microswitches,¹⁵ and microfilters¹⁶ are examples of devices utilizing BCB.

With few exceptions, the implementation of CYCLOTENE in MEMS has been mainly limited to packaging¹⁷ and adhesive bonding.^{18,19} Some preliminary studies on mechanical properties,^{20,21} optical properties,²² and electrical properties²³ of thin film CYCLOTENE have now enabled its application as a MEMS material. As an example, a CYCLOTENE diaphragm has been used for its low thermal conductivity and mechanical robustness in a MEMS-based infrared detector.²⁴

^{a)} Author to whom correspondence should be addressed; electronic mail: ghodssi@eng.umd.edu

The advantages of using a low- k dielectric, as an insulating layer, with excellent mechanical and electrical properties, make CYCLOTENE attractive for MEMS devices. However, any new material should be compatible with the MEMS fabrication processes. One of the key MEMS fabrication technologies is bulk micromachining. Anisotropic etching of silicon by alkali hydroxide etchants like potassium hydroxide (KOH) is one of the most common and efficient bulk micromachining techniques.²⁵ Etching processes with KOH solutions can be tuned to provide the desired etch rate with relatively low surface roughness and high etch selectivity between $\langle 100 \rangle$ and $\langle 111 \rangle$ planes.²⁶ Highly doped silicon can also be used as an etch stop layer.²⁷ Structures with a fixed angle of 54.74° are etched in $\langle 100 \rangle$ silicon. Such anisotropic etching is either a part of backside etching process to release membranes for sensor applications^{28,29} or front side etching to fabricate grooves in silicon as microfluidic channels,³⁰ housing for optical fiber,³¹ or microball bearings.^{32,33}

CYCLOTENE, like other organic materials, has poor interfacial fracture resistance (adhesion) to inorganic materials.³⁴ The poor adhesion becomes a major problem when processes like wet etching in corrosive chemicals need to be performed after CYCLOTENE deposition. The metal film peels off from the inorganic substrate after exposure to specific chemicals used in fabrication process and the CYCLOTENE film might get attacked or etched in the corrosive solution. We have shown that fabrication of deep silicon etched structures together with CYCLOTENE dielectric films can be performed using appropriate metal etch masks with modified process flow to enhance the metal/CYCLOTENE adhesion.

II. TEST STRUCTURES

Integration of CYCLOTENE film and wet bulk micromachining of silicon (KOH) is performed using a metal etch mask scheme. Schematic cross section of fabricated structures is shown in Fig. 1. Silicon nitride, CYCLOTENE film, and metal are deposited and patterned on a silicon substrate. Silicon nitride (SiN_x) is used as a backside KOH etch mask. The silicon is then etched in KOH solution.

Au is used as an etch mask due to its insignificant etch rate in KOH³⁵ [some other silicon etchants used in bulk micromachining like tetra methyl ammonium hydroxide, ethylene diamine pyrochatechol, and xenon difluoride are also gold selective]. Since Au has inherently poor adhesion to most polymers,³⁶ a thin Cr film is used as adhesion layer between Au and CYCLOTENE. Metal is deposited at temperatures below the glass transition temperature ($\sim 350^\circ\text{C}$) of CYCLOTENE.

Silicon has an etch rate of $\sim 0.9\ \mu\text{m}/\text{min}$ in 20 wt% (% by weight), 72°C , KOH solution³⁷ in which the exact rate is a function of temperature, concentration, and agitation of the etchant solution. KOH concentration below 20% results in rough etched surfaces and the formation of potential insoluble residues. Concentration higher than 30% results in the formation of vertical $\langle 100 \rangle$ crystal planes on a $\langle 100 \rangle$ wafer.³⁷ Therefore a 20–30 wt% concentration results in less

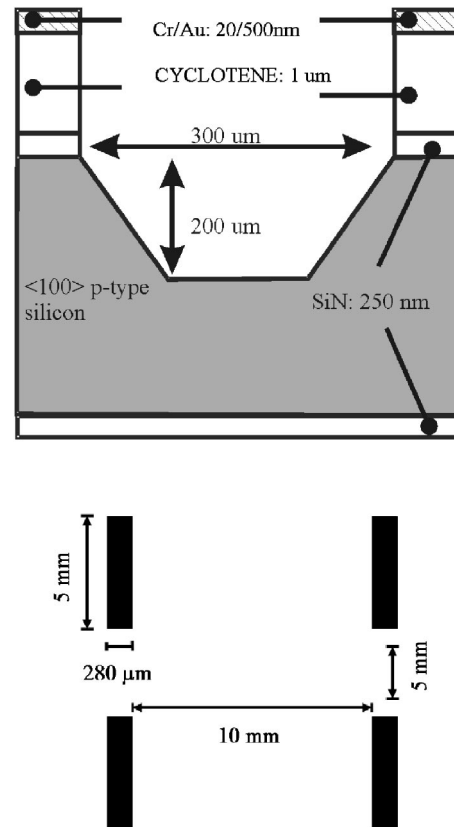


FIG. 1. (Color online) (a) Cross section schematic of desired structure. SiN_x , CYCLOTENE and Cr/Au are deposited first. Metal is patterned, CYCLOTENE and SiN are etched in plasma etcher, and Si is etched in KOH. CYCLOTENE layer is masked by Cr/Au during Si etch process. (b) Schematic top view of test structures. The dimensions are not to scale.

rough etched surfaces. KOH is extremely corrosive and attacks CYCLOTENE as well as metals like Cr, Al and titanium (Ti).^{35,38} The etch rate of Cr in KOH (30 wt%, 80°C) is reported to be around $4.2\ \text{nm}/\text{min}$.³⁵ During long and harsh KOH etching the integrity of all parts of the MEMS devices, especially low- k polymer, needs to be preserved. This integrity includes preserving electrical properties, like dielectric constant and breakdown voltage, as well as mechanical robustness of the film. Depending on the desired etch depth and other etch characteristics, silicon is typically etched for a few hours in KOH solution. Fabrication of deep trenches by bulk micromachining, in most cases, is performed after the fabrication of thin film structures mainly because planarization of the deeply etched trenches is not always possible. After short exposure of Cr/Au film to hot KOH, the metals peel off from the underlying CYCLOTENE. This is due to loss of adhesion in corrosive solution. Therefore it is necessary to fabricate structures with very strong adhesion between metal and polymer to prevent any metal peel-off during the long KOH etching.

III. FABRICATION PROCESS

Low stress silicon nitride is deposited on both sides of a 100-mm-diam p -type silicon wafer (2500 Å thick with residual stress of 250–300 MPa). The wafer is dehydrated at

125 °C for 10 min. Adhesion promoter AP3000™ from Dow Chemical is applied onto the wafer to improve the adhesion of CYCLOTENE to the substrate and a 1- μm -thick CYCLOTENE 3022-35 film is spun at 3000 rpm and cured at 210 °C for 40 min in an N_2 environment. This curing step is known as a soft cure. AP3000 is then spun at 3000 rpm on soft cured CYCLOTENE. The wafer is dehydrated and put inside the ATC 1800-V magnetron sputtering tool (AJA International, N. Scituate, MA). The temperature is ramped using the substrate heater at 1.6 °C/min up to 200 °C in about 1×10^{-7} Torr vacuum. Direct Current sputtering of 200 Å Cr and 0.5 μm Au is performed at 200 °C. The wafer is then cured at 250 °C for 1 h at 1×10^{-7} Torr inside the sputtering chamber. The test wafers, prepared as above, were tested by conventional pull in tape adhesion test. None of the fabricated wafers failed the tape test. The wafers were then patterned by a lithography process with 10 μm AZ9245 positive photoresist. The Au was etched using a commercial Au etchant (type TFA from Transene Inc.). The Cr was wet etched using a commercial Cr etchant (type A from Transene Inc.). The CYCLOTENE was etched in a plasma etcher at a rf power of 100 W, pressure of 250 mTorr, O_2 flow rate of 90 sccm and CF_4 flow of 10 sccm with an etch rate of 0.6 $\mu\text{m}/\text{min}$. The photoresist was then stripped. The samples were (total of 28 grooves on wafer) etched 200 μm deep in 20 wt%, 80 °C KOH solution for 8 h. The solution was aggressively agitated by magnetic stirrer.

IV. EXPERIMENTAL RESULTS

The idea of masking the CYCLOTENE with metal only works if the adhesion between Cr and CYCLOTENE is strong and not affected during KOH etching. Figure 2(a) shows the device with metal peeled off from the polymer after short etching. This device was fabricated by Cr/Au metallization on hard cured CYCLOTENE film. In order to improve a weak adhesion, we have tried different techniques. The most common technique is the surface treatment of CYCLOTENE prior to metallization. In the past, different techniques have been implemented for a surface treatment of CYCLOTENE. Ultraviolet/ozone treatment is believed to increase the surface tension and improve the adhesion of CYCLOTENE to underfill.³⁹ It is also believed that this treatment forms a near- SiO_2 composition at the surface and degrades the polymer structure.⁴⁰ Low energy (3–6 KeV) N_2^+ beams and N_2 plasma were reported to improve the adhesion of Cu to CYCLOTENE.^{41,42} N_2 plasma improves the CYCLOTENE/ SiO_2 adhesion.⁴³ Adhesion of evaporated Cu was improved by the pre-deposition treatment of the CYCLOTENE surface with Argon ion (Ar^+) sputtering. Adhesion improvement is known to be due to chain fragmentation and loss of electron delocalization.⁴⁴ Tuning the sputtering process in which Ar acts as both the carrier gas and the sputtering ion improves Ti and Cu adhesion to CYCLOTENE.⁴⁵ Plasma etching of CYCLOTENE with O_2 and halogen gases (Cl_2, F_2) also modifies the surface^{3,46} and

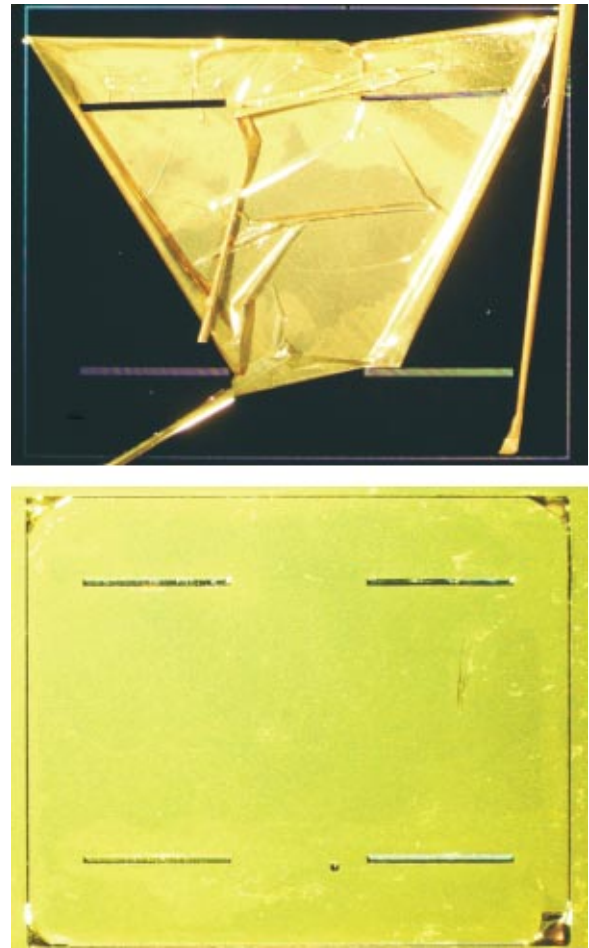


Fig. 2. (Color online) Optical micrograph of a die with $\text{SiN}_x/\text{CYCLOTENE}/\text{Cr}/\text{Au}$ films etched in a 20 wt%, 80 °C KOH solution. (a) The metal layers were peeled off after 10 min exposure to KOH and underlying CYCLOTENE layer was attacked by KOH. Sample was prepared by metal deposition on hard cured CYCLOTENE. (b) Shows negligible metal peel-off after 8 h of etching. The CYCLOTENE film was soft cured and covered with AP3000 prior to metallization, and hard cured afterwards.

plays a role in adhesion improvement. Reactive ion etching with O_2/N_2 was also found to be useful prior to Cr and Cu evaporation.⁴⁷

We have found that a short (1 min) O_2 plasma significantly improves the adhesion of Cr to fully cured (250 °C, 1 h) CYCLOTENE. O_2 plasma is believed to oxidize the surface of CYCLOTENE and form a near- SiO_2 surface which results in better adhesion with Cr. O_2 plasma was performed for 1 min in a plasma etcher at a-rf power, pressure, and flow rate of 150 W, 500 mTorr, and 50 sccm, respectively. Longer or shorter plasma treatments did not cause significant adhesion improvement. O_2 plasma prior to metallization is more effective if it is performed in the metal deposition chamber (to avoid vacuum breaking between the surface treatment and metallization step) but this was not practical in our case. Further studies on adhesion improvement resulted in developing a fabrication technique that provided better adhesion compared to an O_2 plasma treatment. Therefore, O_2 plasma, as explained later, was not used in the final device fabrication.

TABLE I. (Color online) Coefficient of thermal expansion (CTE) of materials used in the test structure.

Material	Si	Cr	Au	CYCLOTENE
CTE, ppm/°C	2.8	6.2	14.4	52

By cure management of CYCLOTENE prior to and after metallization and by using adhesion promoter, we have been able to fabricate metal/CYCLOTENE structures which have excellent adhesion. First, the CYCLOTENE is partially cured which results in $\sim 75\%$ cross-linking of the polymer.⁴⁸ The cure should be performed at a temperature and time period that drives out all the solvent inside the film. Full cross-linking (polymerization) of CYCLOTENE at 250 °C after metallization allows a partially cross-linked CYCLOTENE to bond to Cr. High-temperature metallization also improves the adhesion. Experimental results show that high-temperature deposition of Cr/Au on CYCLOTENE results in better adhesion possibly due to the higher surface energy of CYCLOTENE and metal atoms at elevated temperature that enhances the cross-linking and bonding process. Although high-temperature metal deposition increases the thermal stress of the metal, which may degrade the adhesion, Cr/CYCLOTENE adhesion did not degrade from the increased thermal stress. Thermal stresses are caused by the difference in the coefficient of thermal expansion (CTE) of the films and the difference between deposition temperature and room temperature. The CTE of these thin films is shown in Table I.

We have used adhesion promoter AP3000 as an intermediate adhesion layer between Cr and partially cured CYCLOTENE. Deposition of AP3000, after soft cure and prior to sputtering of Cr/Au, improves the adhesion. AP3000 (Vinyltriacetoxysilane) is a silane-based adhesion promoter which is normally used as primer on substrates prior to spin coating CYCLOTENE and not on the partially cured CYCLOTENE. The role of cure management and AP3000 adhesion promoter in improving the adhesion is investigated by interface analysis techniques which are discussed in Sec. V. Using O₂

plasma prior to AP3000 deposition did not improve the adhesion. Therefore O₂ plasma was not used in the final device fabrication.

Fabricated test structures, described in Sec. III, were etched in 20 wt%, 80 °C KOH solution for 8 h. Figure 2(b) shows the optical micrograph of the etched device. Scanning electron micrographs (SEMs) of the cross section of etched structures are shown in Fig. 3. The figures show a 200- μm -deep etched silicon v-shaped groove in the presence of 1 μm CYCLOTENE which was protected by Au film during the 8 h of KOH etching. The optical and SEM pictures show negligible CYCLOTENE peel-off from the edges of the wafer and edges of the opening pattern (v-groove wall). Shorter etch time results in less or no lateral peel-off.

V. INTERFACE STUDY

To understand the role of cure management and adhesion promoter in improving adhesion, the interface chemistry of the CYCLOTENE/Cr/Au was studied. Previous studies on Cr/CYCLOTENE adhesion and their interface have confirmed the formation of chromium oxide at the interface of metal-polymer.^{49,50} It was reported that the Cr/CYCLOTENE interface is irregular. Cr is diffused and therefore detected inside the CYCLOTENE layer. Cr concentration increases only after annealing at 250 °C for 17 h. For such a long annealing time, formation of CrSi₂ was reported.

We have correlated the adhesion improvement obtained experimentally to the diffusion and chemistry change at the interface due to the cure management of CYCLOTENE and use of AP3000 adhesion promoter.

A. Sample preparation

Samples consisted of 100-mm-diam, 550- μm -thick, silicon wafers with blanket films of CYCLOTENE, Cr, and Au. Table II shows the summary of interface study samples fabricated for this purpose. The CYCLOTENE films were measured to be about 1 μm thick on all samples. Soft cure and hard cure were done at 210 °C for 40 min, and 250 °C for 1 h in the N₂ environment, respectively. A thin film of Cr (20

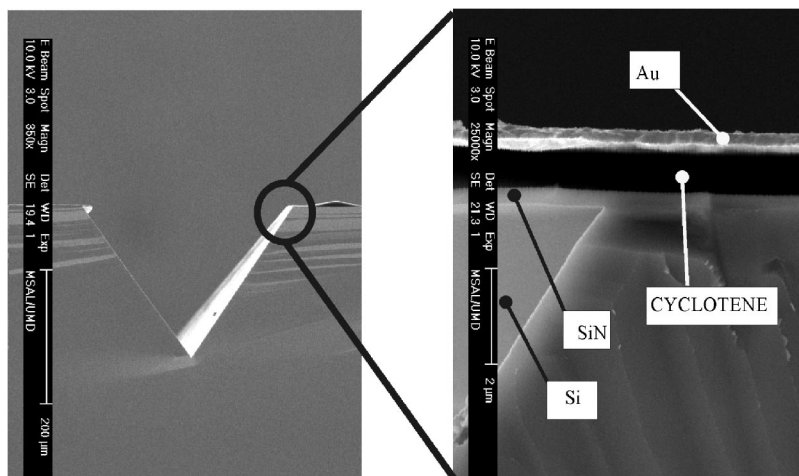


FIG. 3. (Color online) Scanning electron micrograph (SEM) of the cross section of the etched silicon structure in presence of CYCLOTENE and metal mask. CYCLOTENE was protected by metal mask during 8 h KOH etching.

TABLE II. (Color online) Interface study samples.

Sample number	Deposited films and process details
I	Cr/Au
II	Cr/Au, cure at 250 °C
III	CYCLOTENE (soft cured)/Cr
IV	CYCLOTENE (soft cured)/AP3000/Cr
V	CYCLOTENE (soft cured)/Cr, cure at 250 °C
VI	CYCLOTENE (soft cured)/AP3000/Cr, cure at 250 °C
VII	CYCLOTENE (soft cured)/Cr/Au
VIII	CYCLOTENE (soft cured)/Cr/Au, cure at 250 °C

nm) and Au (0.5 μm) was deposited by e-beam evaporation. The thickness of Cr and Au was chosen based on the developed masking process explained earlier in Sec. IV.

B. Cr and Au diffusion

Time of flight secondary ion mass spectroscopy (ToF-SIMS) was used to investigate the Cr diffusion into Au after Au deposition and cure at 250 °C for 1 h. This was performed using a 5 keV O_2^+ sputtering beam together with a 25 keV Ga^+ primary beam for data acquisition. To minimize the resolution loss by crater edge effects, the ratio of sputtered/analyzed area was set to be 10. The mass resolution was higher than 4500 at ^{28}Si . Figure 4 shows the depth profiles of samples I and II. The profiles are given for Au, Cr, and Si in these plots. Figure 4(a) shows that Cr diffusion into Au layer, as deposited, is negligible. However, the Cr signal intensity, as shown in Fig. 4(b), increases by three orders of magnitude after cure.

The quantitative value for Cr concentration at the gold film was obtained using Auger electron spectroscopy (AES). Depth profiling was performed using a 3 keV Ar^+ sputtering beam, together with a 3 keV electron beam for data acquisition. Figure 5 shows the AES depth profiles for these samples. From these results, Cr concentration at the gold layer was estimated to be on average about 1 at. %. The calculation was done using tabulated sensitivity factors.

To investigate the lateral distribution of Cr inside the Au layer, high lateral resolution ToF-SIMS images was acquired on sample II. This was done using a finely focused 25 keV Ga^+ beam. The mass resolution of this method is about 500 at ^{28}Si and the lateral resolution is about 0.2 μm . The analysis was done after mild sputtering of the surface for 1 min to remove surface contamination (the complete removal of the film required 30 min sputtering). The analysis is undertaken after exploiting various analytical approaches to maximize signal intensity. Simultaneous detection of Cr and Au ions is biased by conflicting ion yields. Cr could be detected as Cr^+ , while Au could be detected as Au^- .⁵¹ Sputtering with O_2^+ and detecting negative signals allows simultaneous detection of Cr and Au in the oxide form of MO_x^- with averaged efficiency. The lateral distribution maps of CrO_4^- , AuO_2^- , together with the superposition of these signals, and $\text{AuO}_2^-/\text{CrO}_4^-$ ratio, and $\text{CrO}_4^-/\text{AuO}_2^-$ ratio are shown in the five images of Fig. 6. It was found that Cr diffusion (after curing) into Au

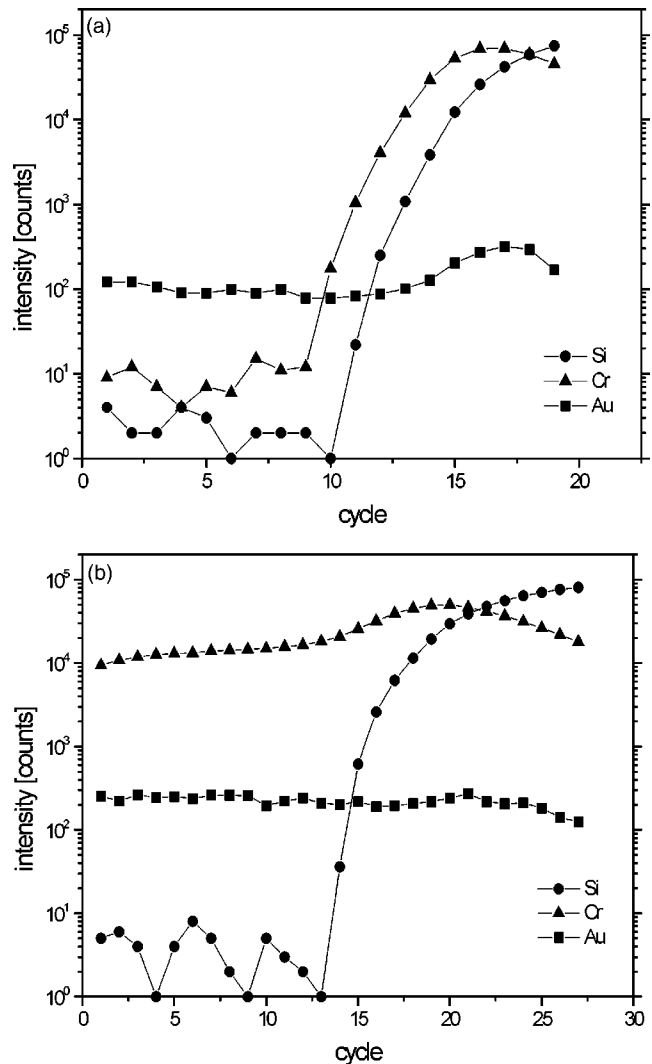


FIG. 4. (Color online) ToF-SIMS depth profiles of samples I and II. (a) Shows insignificant Cr concentration at the Au surface of sample I. (b) Shows three orders of magnitude Cr signal intensity increase after curing at 250 °C for 1 h for sample II. Curing has caused the Cr diffusion into Au.

layer is not homogeneous. Chromium-enriched grains of 2 μm or smaller were detected close to pure Au grains.

The diffusion of Cr into Au could deteriorate the masking strength of the Au against KOH solution which ultimately may cause the formation of pin holes in the Au film during the KOH etching process. However, the Cr grains inside the Au layer are irregular and have small concentration. It is expected that Cr diffusion will have insignificant effect on masking strength of the Au. This argument is supported by the experimental results discussed in Sec. IV, but since Cr diffusion is temperature and time dependent, further cure of the films (above 250 °C for 1 h) may deteriorate the Au masking function.

C. Cr/Cyclotene interface

The second part of the study concentrates on the effect of adhesion promoter at Cr/CYCLOTENE interface as well as the effect of cure before and after metallization. As men-

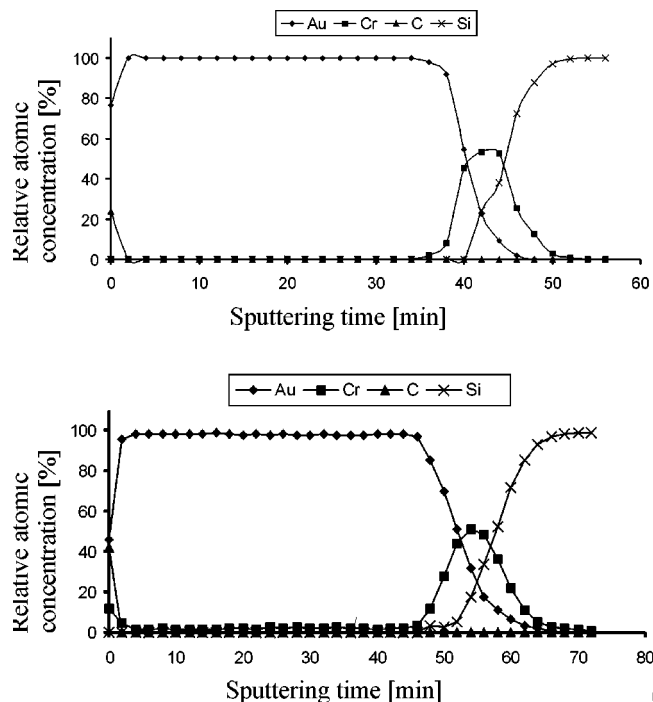


FIG. 5. (Color online) AES depth profile of sample I (a) and II (b) is performed to quantify the Cr concentration at Au surface. Cr concentration was found to be 1 at. % at the Au surface.

tioned in Sec. IV, it was found that covering the partially cured CYCLOTENE with AP3000 prior to metallization, followed by full curing of the film, drastically improves the adhesion. Previous studies do not provide a clear picture of the role of AP3000 adhesion promoter at the interface of CYCLOTENE and other inorganic materials,^{34,52} however, it was experimentally proven that using AP3000 at the interface of CYCLOTENE and other inorganic materials such as silicon, silicon nitride, Al, Cu, and TiW improves the adhesion of this polymer significantly.^{52,53} The molecular structure of CYCLOTENE⁵⁴ and AP3000⁵⁵ are shown in Fig. 7. The thickness of the adhesion promoter measured by different techniques is reported to be approximately 15 nm by Im *et al.*⁵² and 0.5–5 nm by Topper, Achen and Reichl.⁵³ The small thickness of this film, together with the fact that the

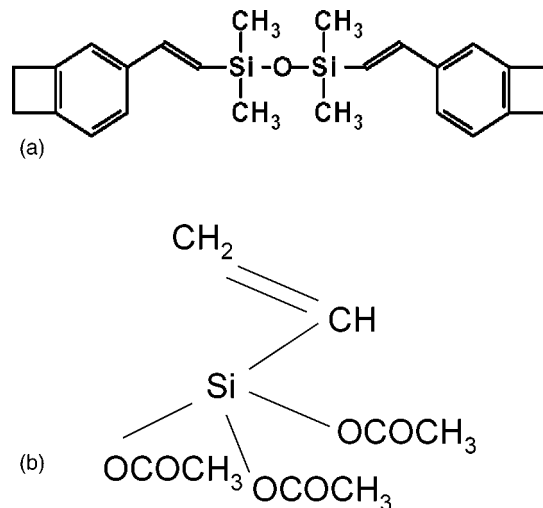


FIG. 7. (Color online) Molecular structure of (a) CYCLOTENE monomer, (b) AP3000 (Vinyl-triacetoxy-silane) adhesion promoter.

molecular structures of CYCLOTENE and AP3000 are close to one another, makes the interface study difficult.

Samples III, IV, V, and VI, listed in Table II, were fabricated for this purpose and analyzed by ToF-SIMS. Due to similar chemical structure of CYCLOTENE and AP3000, the markers of AP3000 on CYCLOTENE are not unique; however, they are distinguishable by comparing the signal intensity of different species of samples III and IV. The results from positive ToF-SIMS, performed using a low energy Ar^+ sputtering beam, are shown in Fig. 8. The two samples are identical except that AP3000 was deposited on sample IV prior to metallization.

From the depth profiles of Fig. 8 it is seen that the intensity of specific species (CrSiO , CrO , Si , SiH , and SiO) in the Cr layer is increased on average about 2–6 times in sample IV, compared to III. The increased intensity in these signals is correlated to the existence of AP3000. The irregular Cr profile on both samples is due to the higher oxygen concentration at the Cr surface as well as the interface for both samples. The signal intensity of Cr is biased by oxygen in this method. The higher the oxygen concentration, the higher is the probability of positive ion formation, and therefore, the

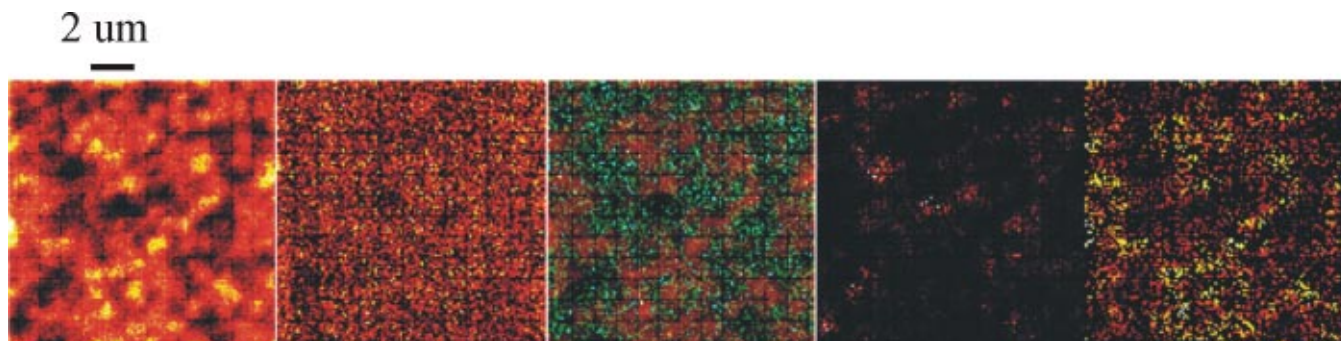


FIG. 6. (Color online) High resolution ToF-SIMS images show lateral distribution of Cr and Au ions of sample II. From left to right: (a) Cr (116: CrO_4^-), (b) Au (229: AuO_2^-), (c) superposition of the first two (CrO_4^- in red, AuO_2^- in cyan), (d) $\text{AuO}_2^-/\text{CrO}_4^-$ ratio, and (e) $\text{CrO}_4^-/\text{AuO}_2^-$ ratio. The field of view is $15 \times 15 \mu\text{m}^2$ and lateral resolution is about 0.2.

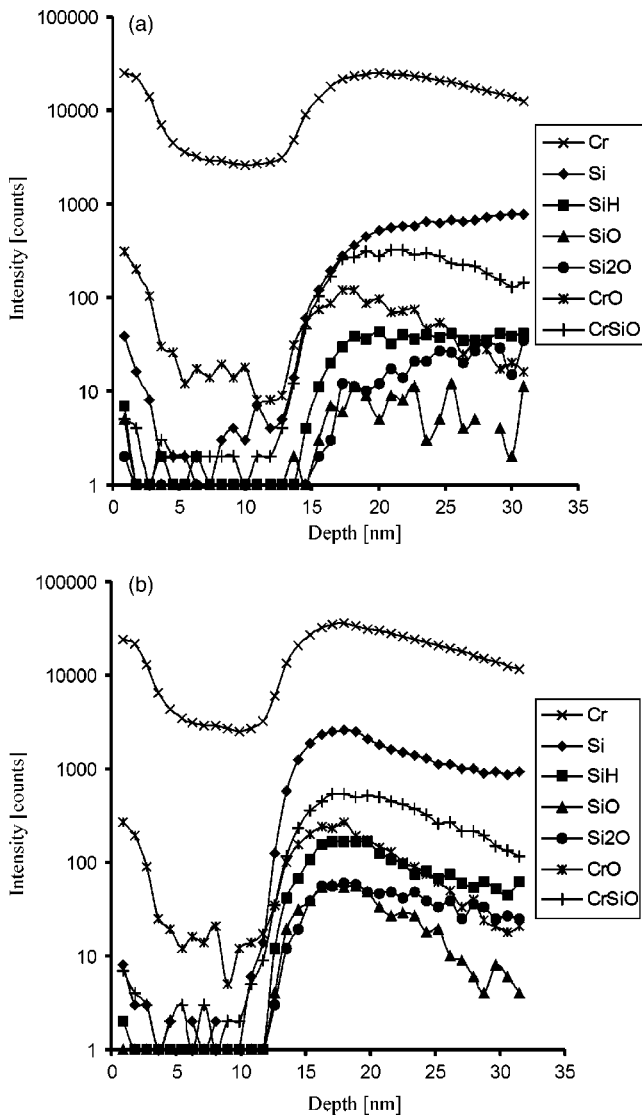


Fig. 8. (Color online) Positive SIMS profile of (a) sample III, (b) sample IV. The profile of Cr, Si, CrSiO, CrO, and SiH are shown. Adhesion promoter track marks are detected.

higher the Cr signal intensity will be. From both graphs it is observed that the oxygen concentration is higher at the Cr surface (Cr oxidizes at the surface). The intensity of the Si signal is also not independent from oxygen concentration. That explains the higher Si concentration at the surface for samples III and IV. The Cr profile shows variations that are not related to the actual change in the materials stoichiometry; however, the species related to the AP3000 are detected from these profiles (Fig. 8).

In order to address the above issue, positive ToF-SIMS by Ar^+ sputtering, together with O_2 flooding of the sample, was performed. This technique allows minimizing the signal intensity variations due to elimination of dependability of the Cr signal to oxygen concentration. Figure 9 shows the depth profiles of different species including Si, SiO, SiH, SiOH obtained using this method for samples III–VI. Figure 9(a) shows depth profiles of samples III and IV, and Fig. 9(b) shows depth profiles of V and VI. The signal intensity of Cr

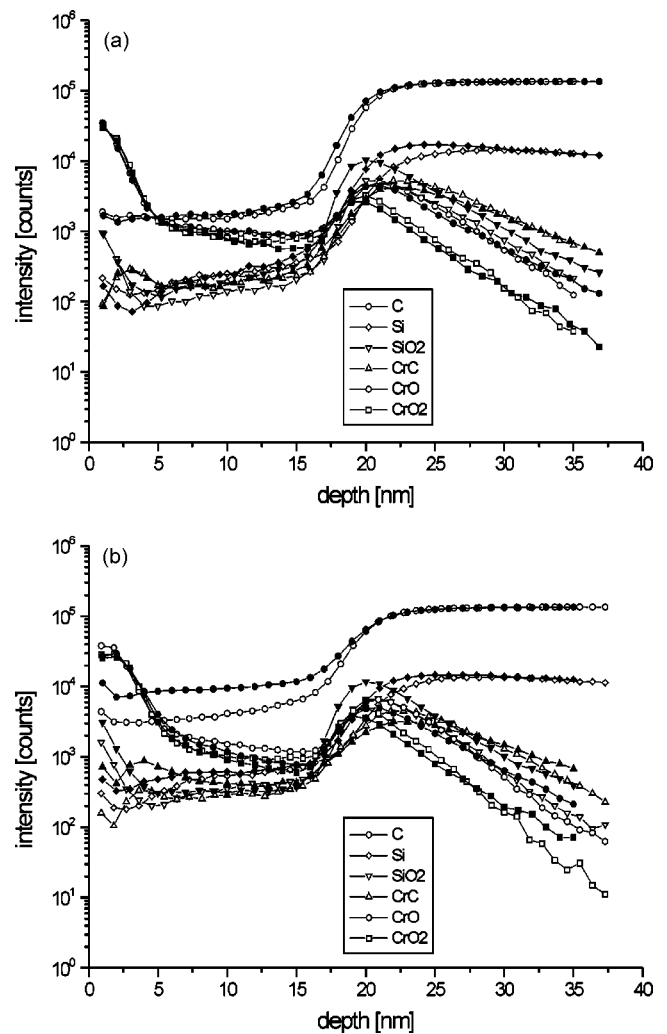


Fig. 9. (Color online) Positive ToF-SIMS depth profiles with Ar^+ sputtering together with O_2 flooding of (a) samples III (unfilled graph) and IV (filled graph), (b) samples V (unfilled graph) and VI (filled graph). Diffusion of Si into Cr layer after hard curing is enhanced by using AP3000.

is the same for all four profiles. This allows us to compare the intensity of other species (like Si) from different profiles to evaluate the stoichiometry of the interface. The results obtained by this method are in good agreement with previous results. The Cr signal intensity is the same for all the profiles and the sensitivity is 20 times higher than previous results shown in Fig. 8. The Si signal intensity (from CYCLOTENE or AP3000 backbone) inside the Cr layer is 10 counts/cycle in samples III and IV, 40 counts/cycle in sample V, and 100 counts/cycle in sample VI. This shows that curing has caused the diffusion of Si into Cr layer. AP3000 enhances the diffusion of Si into Cr, too [Fig. 9(b)]. It is believed that Si diffusion into Cr, due to the cure and use of AP3000, is one of the contributing factors for improving the adhesion. From the profiles of Fig. 9, it is seen that along with Si, the intensity of SiH, SiO, and SiOH signals has also increased inside the Cr layer.

Figure 10 shows the negative ToF-SIMS depth profiles performed with a 3 keV Cs^+ sputtering beam. Figure 10(a)

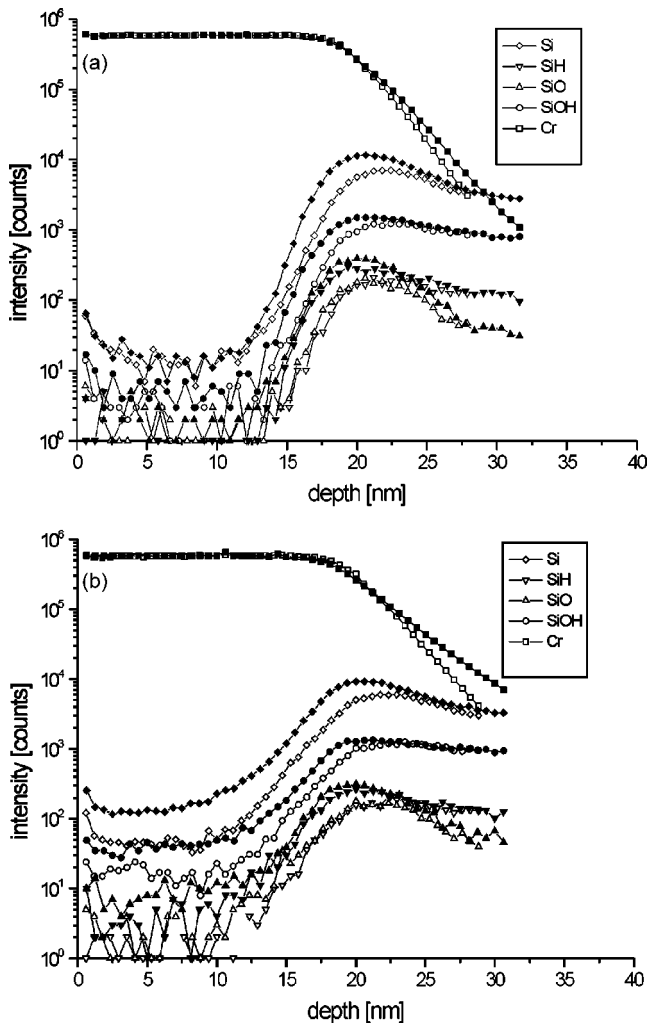


FIG. 10. (Color online) Negative ToF-SIMS depth profiles with Cr^+ sputtering of (a) samples III (unfilled graph) and IV (filled graph), (b) samples V (unfilled graph) and VI (filled graph). Cr is oxidized at the interface and diffusion of C into Cr layer after hard curing is enhanced by using AP3000.

shows depth profiles of samples III and IV, and Fig. 10(b) shows depth profiles of V and VI. Depth profiles of Si, SiO_2 , CrC, carbon (C), CrO, and CrO_2 are shown in these two graphs. Carbon concentration is very similar on samples III and IV, but increases on sample V and finally is the highest on sample VI. Diffusion of C into the Cr layer is significantly increased after the cure at 250 °C for 1 h in sample VI. This suggests that the use of either AP3000 or a cure by itself does not significantly enhance the diffusion of C. However, it is the combination of these factors that enhance the diffusion. Diffusion of C into Cr is therefore the other reason for adhesion improvement. Partial cross-linking of CYCLOTENE during the soft cure and before metallization facilitates the diffusion of Si and C atoms into the Cr layer after curing at 250 °C for 1 h.

Figure 10 shows that from 10 nm beneath the Cr surface, the signal intensity of chromium oxide species (CrO^- and CrO_2^-) increases towards the Cr surface and the interface. The increased intensity of CrO^- and CrO_2^- at the interface confirms the previous results shown in Fig. 8 for the Cr oxida-

tion. The intensity of CrO^- , CrO_2^- , and SiO_2 has increased near the surface after curing. This shows the chemical reaction of CYCLOTENE or AP3000 with the Cr layer. It is believed that the oxidation process is a contributing factor to the adhesion improvement between Cr and CYCLOTENE due to cure of the film. The interface analysis results (shown in Figs. 8–10) provide valuable information on the role of AP3000 at the metal/polymer interface as well as the effect of soft cure (before metallization) and hard cure (after metallization).

VI. CONCLUSION

A fabrication process for the integration of CYCLOTENE and the wet etching of silicon by KOH was developed. This allows fabrication of highly efficient MEMS micromachines using CYCLOTENE as a low- k dielectric material. Adhesion improvement of CYCLOTENE and the Cr/Au mask was accomplished by partial cure of the CYCLOTENE prior to metallization, sputtering of the Cr/Au metal masks at 200 °C, and full curing at 250 °C. Adhesion promoter, AP3000, was proven to enhance the adhesion of these films if applied prior to metallization. Metal/CYCLOTENE adhesion was tested to be very strong. Deep structures (200 μm) in silicon were fabricated while the CYCLOTENE film was protected by a metal mask. Long exposure to KOH solution (8 h) had little or no effect on the adhesion of the polymer-metal. The process was repeatable with the same set of results. In order to understand the effect of soft cure and the adhesion promoter prior to metallization and hard cure after metallization, the metal/CYCLOTENE interface was studied. It was found that curing at 250 °C, together with use of adhesion promoter on partially cured CYCLOTENE, results in diffusion of silicon and carbon from CYCLOTENE or AP3000 or both into the Cr layer. The chemical interaction of CYCLOTENE and Cr at the interface mainly in the form of oxidation of Cr was observed, too. The above phenomena are correlated to the adhesion improvement.

ACKNOWLEDGMENTS

This work was supported by the National Science Foundation under Grant No. ECS-0224361, the Minta Martin Foundation, and the Small Smart Systems Center at the University of Maryland. The authors would like to thank Thomas C. Loughran and Nolan A. Ballew from the University of Maryland (UMD) clean room facilities for their help with fabrication of devices as well as Erica Jacob from ITC-irst for her help with AFM pictures and Wen-Hsien Chuang from MEMS Sensors and Actuators Lab at UMD for help with SEM pictures.

¹R. A. Kirchhoff and K. J. Bruza, *Prog. Polym. Sci.* **18**, 85 (1993).

²M. F. Farona, *Prog. Polym. Sci.* **21**, 505 (1996).

³P. B. Chinoy and J. Tajadod, *IEEE Trans. Compon., Hybrids, Manuf. Technol.* **16**, 714 (1993).

⁴A. J. G. Strandjord, R. H. Heistand, P. Garrou, and T.G. Tessier, *44th Electronic Components and Technology Conference, May 1994*, Washington, DC, p. 374.

⁵D. C. Burdeaux, P. H. Townsend, J. N. Carr, and P. Garrou, *J. Electron. Mater.* **19**, 1357 (1990).

- ⁶M. J. Berry, T. G. Tessier, I. Turlik, G.M. Adema, D.C. Burdeaux, J.N. Carr, and P. Garrou, *40th Electronic Components and Technology Conference, May 1990*, Las Vegas, NV, p. 746.
- ⁷Y. Ida, P. E. Garrou, A. J. G. Strandjord S.L. Cummings, W.B. Rogers, M.J. Berry, and S.R. Kisting, *8th IEEE/CPMT International Electronic Manufacturing Technology Symposium, Dec. 1995*, Omiya, Japan, p. 441.
- ⁸L. A. Keser, R. Bajaj, and T. Fang, *IEEE Trans. Adv. Packag.* **23**, 3 (2000).
- ⁹D. T. Price, R. J. Gutmann, and S. P. Murarka, *Thin Solid Films* **308**, 309, 523 (1997).
- ¹⁰A. J. G. Strandjord, W. B. Rogers, Y. Ida, R.R. De Vellis, S. Shiau, E.S. Moyer, D.M. Scheck, and P.E. Garrou, *47th Electronic Components and Technology Conference, May 1997*, New York, New York, p. 1260.
- ¹¹X. Huo, K. J. Chen, and P. C. H. Chan, *Proceedings of the 2002 International Microwave Symposium, June 2002*, Seattle, WA, Vol. 1, p. 513.
- ¹²C. F. Kane and R. R. Krchnavek, *IEEE Photonics Technol. Lett.* **7**, 535 (1995).
- ¹³S. Wolff, A. R. Giehl, and M. Renno, *Appl. Phys. B: Lasers Opt.* **73**, 623 (2001).
- ¹⁴C. Laville, C. Pellet, and G. N'Kaoua, *First Annual International IEEE MBS Special Topic Conference, Oct. 2000*, Lyon, France, p. 572.
- ¹⁵H. H. Gatzel, E. Obermeier, T. Kohlmeier T. Budde, H.D. Ngo, B. Mukhopadhyaya, and M. Farr, *TRANSDUCERS '03, June 2003*, Boston, MA, Vol. 2, p. 1514.
- ¹⁶P. Turmezei, A. Polyakov, J. R. Mollinger M. Bartek, A. Bossche, and J.N. Burghartzet, in Ref. 15, Vol. 1, p. 107.
- ¹⁷A. Jourdain, X. Rottenberg, G. Carchon, and H.A. C. Tilmans, in Ref. 15, p. 1915.
- ¹⁸F. Niklaus, H. Andersson, P. Enoksson, and G. Stemme, *Sens. Actuators, A* **A92**, 235 (2001).
- ¹⁹T.-K. A. Chou and K. Najafi, *TRANSDUCERS '01, 2001*, Munich, Germany, Vol. 2, p. 1570.
- ²⁰J. Im, E. O. Shaffer, R. Peters T. Rey, C. Murlick, and R.L. Sammler, *International Symposium on Microelectronics 1996*, Minneapolis, MN, p. 168.
- ²¹J.-h. Im, E. O. Shaffer II, T. Stokich, Jr., *et al.*, *Trans. ASME, J. Electronic Packag.* **122**, 28 (2000).
- ²²J. T. Beechinor, E. McGlynn, M. O'Reilly, G.M.Crean, *Microelectron. Eng.* **33**, 363 (1997).
- ²³A. Modafe, N. Ghalichechian, B. Kleber, and R. Ghodssi, *IEEE Trans. Device Mater. Reliab.* (to be published).
- ²⁴S. Guo, *Proc. SPIE* **4979**, 422 (2003).
- ²⁵H. Seidel, L. Csepregi, A. Heuberger, and H. Baumgartel, *J. Electrochem. Soc.* **137**, 3612 (1990).
- ²⁶G. T. A. Kovacs, N. I. Maluf, and K. E. Petersen, *Proc. IEEE* **86**, 1536 (1998).
- ²⁷H. Seidel, L. Csepregi, A. Heuberger, and H. Baumgartel, *J. Electrochem. Soc.* **137**, 3626 (1990).
- ²⁸N. Yazdi, F. Ayazi, and K. Najafi, *Proc. IEEE* **86**, 1640 (1998).
- ²⁹W. P. Eaton and J. H. Smith, *Smart Mater. Struct.* **6**, 530 (1997).
- ³⁰R. Nayve, M. Fujii, A. Fukugawa, and M. Murata, *IEEE Sixteenth Annual International Conference on MEMS, Jan. 2003*, Kyoto, Japan, p. 456.
- ³¹C. Strandman and Y. Backlund, *J. Microelectromech. Syst.* **6**, 35 (1997).
- ³²R. Ghodssi, D. D. Denton, A. A. Seireg, and B. Howland, *J. Vac. Sci. Technol. A* **11**, 803 (1993).
- ³³T. W. Lin, A. Modafe, B. Shapiro, and R. Ghodssi, *IEEE Trans. Instrum. Meas.* **53**, 839 (2004).
- ³⁴S.-Y. Kook, J. M. Snodgrass, A. Kirtikar, and R.H. Dauskardt, *J. Electron. Packag.* **120**, 328 (1998).
- ³⁵K. R. Williams, K. Gupta, and M. Wasilik, *J. Microelectromech. Syst.* **12**, 761 (2003).
- ³⁶L.-H. Lee, *Fundamentals of Adhesion* (Plenum, New York, 1991), p. 50.
- ³⁷H. Siedel, *TRANSDUCERS '87, 1987*, Tokyo, Japan, p. 120.
- ³⁸U. Munch, O. Brand, O. Paul, H. Baltes, and M. Bossel, *MEMS 2000, Jan. 2000*, Miyazaki, Japan, p. 608.
- ³⁹S. Luo and C. P. Wong, *IEEE Trans. Comput.-Aided Des.* **24**, 43 (2001).
- ⁴⁰B. Viallet, E. Daran, and L. Malaquin, *J. Vac. Sci. Technol. A* **21**, 766 (2003).
- ⁴¹D.-Q. Yang and E. Sacher, *Appl. Surf. Sci.* **195**, 202 (2002).
- ⁴²D.-Q. Yang, L. Martinu, E. Sacher, and A. Sadough-Vanini, *Appl. Surf. Sci.* **177**, 85 (2000).
- ⁴³E. O. Shaffer, M. E. Mills, D. D. Hawn, J.C. Liu, and J.P. Hummel, *Proceedings of the IEEE International Interconnect Technology Conference, June 1998*, San Francisco, CA, p. 223.
- ⁴⁴D.-Q. Yang and E. Sacher, *Appl. Surf. Sci.* **173**, 30 (2001).
- ⁴⁵D.-Q. Yang, E. Sacher, E. M. Griswold, and G. Smith, *Appl. Surf. Sci.* **180**, 200 (2001).
- ⁴⁶M. R. Baklanov, S. Vanhaelemeersch, H. Bender, and K. Maex, *J. Vac. Sci. Technol. B* **17**, 372 (1999).
- ⁴⁷M. J. Berry, I. Turlik, P. L. Smith, and G.M. Adema, *Mater. Res. Soc. Symp. Proc.* **227**, 351 (1991).
- ⁴⁸R. V. Tanikella, S. A. Bidstrup, and P. A. Kohl, *J. Appl. Polym. Sci.* **83**, 3055 (2002).
- ⁴⁹K. W. Paik, R. J. Saia, and J. J. Chera, *Mater. Res. Soc. Symp. Proc.* **203**, 303 (1991).
- ⁵⁰K. W. Paik, H. S. Cole, R. J. Saia, and J.J. Chera, *J. Adhes. Sci. Technol.* **7**, 403 (1993).
- ⁵¹A. Benninghoven, F. G. Radenauer, and H. W. Werner, *Secondary Ion Mass Spectrometry Basic Concepts, Instrumental Aspects, Applications and Trends* (Wiley, New York, 1987).
- ⁵²J. Im, T. Stokich, Jr., J. Hetzner *et al.*, in *Proceedings of the International Symposium on Advanced Packaging Materials, Mar. 1999*, Braselton, GA, p. 53.
- ⁵³M. Topper, A. Achen, and H. Reichl, in *53rd Electronic Components and Technology Conference Proceedings, May 2003*, New Orleans, LA, p. 1843.
- ⁵⁴H. Hendricks, *Mater. Res. Soc. Symp. Proc.* **443**, 3 (1997).
- ⁵⁵J. M. Snodgrass, D. Pantelidis, J. C. Bravman, and R.H. Dauskardt, *Mater. Res. Soc. Symp. Proc.* **565**, 123 (1999).